

MODULATION OF NEAR-WALL ANISOTROPY WITH UNIFORM WALL BLOWING AND SUCTION

Yongmann M. Chung

Department of Engineering, University of Warwick
Coventry CV4 7AL, U.K.
Y.M.Chung@Warwick.ac.uk

Hyung Jin Sung

Department of Mechanical Engineering
Korea Advanced Institute of Science and Technology (KAIST)
373-1 Kusong-dong, Yusong-ku, Taejeon, 305-701, South Korea

ABSTRACT

Direct numerical simulation data have been analysed to investigate the effect of uniform wall blowing and suction on the near-wall turbulence structure. Blowing is applied at the lower wall of the channel and suction at the upper wall, respectively. The modulation of the near-wall anisotropy with uniform wall blowing and suction is examined in terms of the anisotropy invariant map (AIM) for the Reynolds stress anisotropy tensor. It is found that blowing makes the flow more isotropic, enhancing transverse ($\overline{v'^2}$ and $\overline{w'^2}$) components of velocity fluctuations significantly. A significant increase in the anisotropy of the near-wall region is found in the suction case, making the flow approach towards a one-component state in the anisotropy invariant map. The AIM analysis indicates that the relaxation processes of the anisotropy of the near-wall turbulence are different for the blowing and suction cases.

INTRODUCTION

Wall blowing and suction has been encountered in many engineering applications such as turbine-blade cooling, transition delay, and separation prevention (Krogstad and Kourakine, 2000). When a fully-developed turbulent wall-bounded flow is subjected to a sudden wall blowing and suction, there is an initial relaxation from the upstream impermeable wall boundary condition towards an equilibrium state after the step change in wall boundary condition (Smits and Wood, 1985; Bushnell and McGinley, 1989).

To date, most of the studies of wall blowing and suction have concentrated on asymptotic cases.

For these, uniform blowing and suction is applied for a long distance and the effects on the flow investigated after the initial relaxation. Examples of this type of study are the experimental investigations of Antonia et al. (1988), the direct numerical simulations (DNS) of Mariani et al. (1993) and Sumitani and Kasagi (1995), and the large-eddy simulations (LES) of Moin (1982) and Piomelli et al. (1989). Although the effect of asymptotic wall blowing and suction on turbulence is well documented, studies on the downstream relaxation after the wall blowing and suction are relatively scarce (Simpson, 1971; Schildknecht et al., 1979).

It is evident that wall blowing and suction affected primarily the near-wall turbulent structure (Park and Choi, 1999). When wall blowing was applied, streamwise vortical structures in smaller scales was found numerically (Sumitani and Kasagi, 1995). On the other hand, Antonia et al. (1988) observed a more orderly behaviour of low-speed streaks and a greater longitudinal coherence of the low-speed streaks from visualisations of a turbulent boundary layer with uniform suction. The elongation of the low-speed streaks and the suppression of the spanwise meandering motion of the streaks were also observed in a recent DNS (Chung et al., 2000; Chung and Sung 2001). These findings imply that the anisotropy of the near-wall region can be affected significantly by the application of wall blowing and suction.

In this study, DNS data of Chung et al. (2000) are analysed to investigate the structural changes after the sudden application of wall blowing and suction. A fully-developed

turbulent channel flow is subjected to sudden wall blowing and suction following an entrance section (see Fig. 1). Uniform blowing is imposed at the lower wall of the channel and uniform suction at the upper wall. The downstream evolutions of flow structure and the rate of adjustment to a new structure are evaluated in terms of the limiting behaviour of Reynolds stress and the anisotropy tensor. The modulation of the near-wall anisotropy associated with uniform wall blowing and suction is examined in terms of the Reynolds stress tensor and the anisotropy invariant map (AIM) for the Reynolds stress tensor.

NUMERICAL METHODS

In the DNS that provides the data set employed in this analysis, the code of Yang and Ferziger (1993) is used. Here, we only summarise the numerical method briefly. Details regarding the procedures can be found in Yang and Ferziger (1993) and Chung and Sung (1997). They are integrated in time using a fractional-step method (Kim and Moin, 1985). The solution procedure consists of a semi-implicit approach. It uses a low storage, third-order Runge-Kutta method for the nonlinear convective terms and a second-order Crank-Nicholson method for the viscous terms. For spatial discretisation, second-order central differences are used.

In the present study, an incompressible turbulent channel flow between two parallel plates is considered. The Reynolds number is $Re = 2180$, which corresponds to $Re_\tau = 150$ based on the channel half-width h and the wall friction velocity at inlet $u_{\tau_{in}}$. The dimensionless wall transpiration velocity $v_0^+ (= v_0/u_{\tau_{in}})$ is set to be 0.05 and the resultant wall transpiration rate is $v_0/U_m = 0.00344$.

The streamwise and spanwise dimensions of the computational domain are set such that $L_x = 51.2h$ and $L_z = 3h$, respectively. So as to describe the initial relaxation process after the perturbation, the box length in the streamwise direction is made large. The spanwise auto-correlation decays to zero. This suggests that the box size is adequate in the spanwise direction.

Grid refinement is performed until more grid points do not cause any significant differences in the result (Chung and Sung, 2001). A $512 \times 129 \times 64$ grid system is used in the x , y , and z directions, respectively. To resolve the near-wall structure, grid stretching is implemented along the wall-normal direction (y) us-

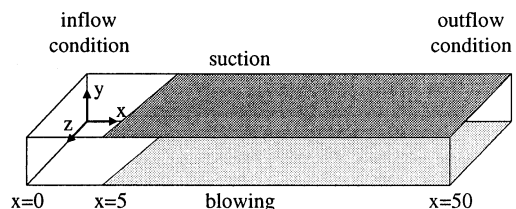


Figure 1: A schematic diagram of flow configuration.

ing a hyperbolic tangent distribution to resolve the near-wall structure. The first grid point away from the wall is located at about $y^+ \approx 0.1$. The streamwise and spanwise grid resolutions are $\Delta x^+ = 15.0$ and $\Delta z^+ = 6.25$, respectively. The time step used is $\Delta t = 0.02h/U_m$, i.e., $\Delta t^+ = 0.2$ in wall units.

RESULTS AND DISCUSSION

To investigate the downstream relaxation of the turbulent structure after wall blowing and suction, the contour lines of the turbulence intensities ($\overline{u'^2}$, $\overline{v'^2}$ and $\overline{w'^2}$) and the Reynolds shear stress ($-\overline{u'v'}$) are shown in Fig. 2. It is known that when a fully-developed turbulent wall-bounded flow is subjected to a sudden wall blowing and suction, there is an initial relaxation from the upstream impermeable wall boundary condition towards an equilibrium state after the step change in wall boundary condition (Smits and Wood, 1985; Bushnell and McGinley, 1989). Although wall blowing and suction is applied from $x = 5$, it is found that there is a delay in the response of the turbulence intensities to the sudden application of wall blowing and suction. As seen, the blowing and suction modify the Reynolds stress significantly. It is evident that blowing enhances the Reynolds stress but suction suppresses it. The response on the blowing side is faster than that on the suction side. After the wall blowing, the turbulence intensities have an increased near-wall peak. At further downstream, the turbulence intensities in the blowing wall reach an equilibrium state, while turbulence intensities in the suction side keep decreasing to the exit of the computational domain. The response of each component of the Reynolds stresses to the wall perturbation is seen to be different from each other, the streamwise component showing the quickest response.

The computational domain size and the grid resolutions are chosen through preliminary simulations (Chung and Sung, 2001). The contours of the three components of the vorticity fluctuations ($\omega_i = \sqrt{\omega_i'^2}$) are demonstrated in Fig. 3. The response of ω_x is similar to those

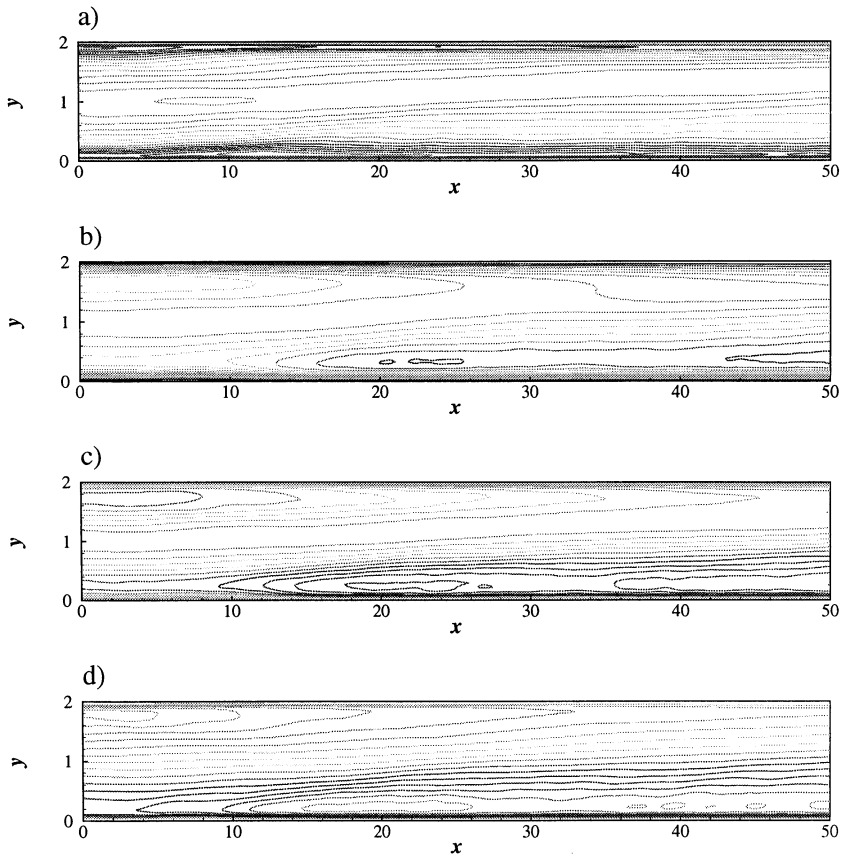


Figure 2: Contours of turbulence intensities. a) u' , b) v' , c) w' , and d) $-\overline{u'v'}$. The increments for u' are 0.01 and 0.005 for elsewhere.

of v' and w' in Fig. 2. The strength of v' and w' increases to the $10h$ downstream after the application of wall blowing. On the contrary, ω_y has an immediate response to the wall blowing and suction. The response of the near-wall turbulent flow to the wall blowing and suction can be explained in terms of the streamwise vortices since the streamwise vortices are closely related with the near-wall turbulent activities. The location of the local maximum ω_x corresponds to the average location of the centre of the streamwise vortices. The average size of the streamwise vortex can be estimated from the distance between the local maximum and minimum (Kim et al., 1987).

A convenient way to characterise flow anisotropy is through the use of the Reynolds stress anisotropy tensor:

$$b_{ij} = \frac{\overline{u'_i u'_j}}{2k} - \frac{\delta_{ij}}{3}, \quad (1)$$

where $k = \overline{u'_k u'_k}/2$ is the turbulent kinetic energy, δ_{ij} is the Kronecker delta and summation over repeated indices is implied. Primes indicate fluctuations about the mean value. In the present study, the Reynolds stress anisotropy

tensor is averaged in the spanwise direction as well as in time and b_{ij} is a function of (x, y) . The second and third invariants of the Reynolds stress anisotropy tensor b_{ij} are given by:

$$II = -\frac{1}{2}b_{ij}b_{ji}, \quad (2)$$

$$III = \frac{1}{3}b_{ij}b_{jk}b_{ki}. \quad (3)$$

Lumley and Newman (1979) have shown that the cross-plots of the invariants $-II$ and III for axisymmetric turbulence and for two-component turbulence define the anisotropy invariant map (AIM) which bounds all physically realizable turbulence. In the AIM, turbulence must exist within the area surrounded by three lines. The upper straight line $II + 3III + 1/9 = 0$ represents a state of two-component turbulence. In general, near the wall, the velocity component normal to the wall (v'^2) is suppressed by the 'splating' phenomenon (Kim et al., 1987) and the anisotropy tensor approaches the line of the two-component state. The right and left boundaries of the AIM ($-II^3/3^3 = III^2/2^2$) identify the prolate and the oblate axisymmetric turbulence

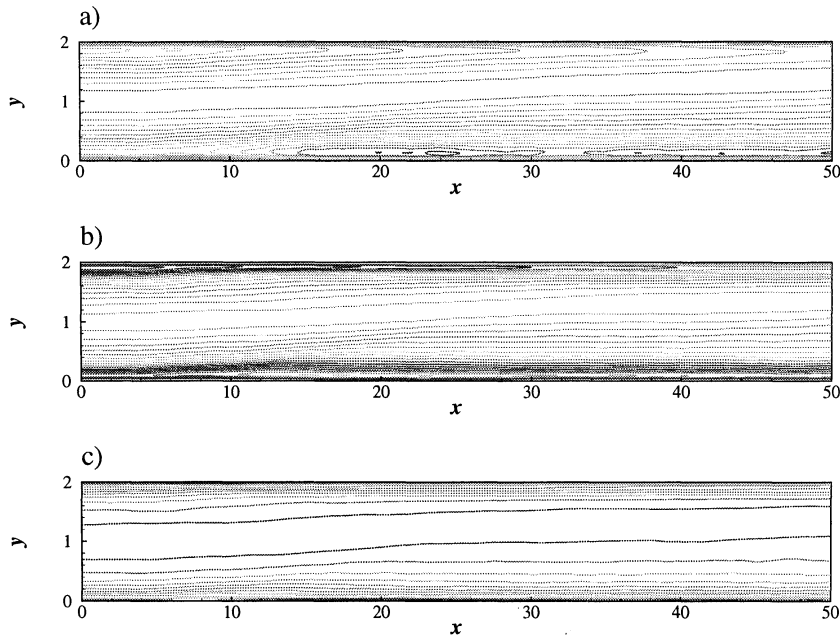


Figure 3: Contours of rms of vorticity fluctuations. a) ω_x , b) ω_y and c) ω_z .

states, respectively. The right vertex of the AIM ($-II = 1/3, III = 2/27$) indicates one-component turbulence. The bottom cusp ($II = 0, III = 0$) characterises the isotropic state of turbulence.

The downstream relaxation of the turbulence anisotropy is examined. The AIMs at three downstream locations ($x = 15$ and 30) are shown in Figs. 4 and 5. It is clearly seen in Fig. 4 that the flow becomes more isotropic when blowing is applied. The early response of the near-wall anisotropy to blowing is substantial. At $x = 15$, the anisotropy data are shifted to the left in the AIM from the inlet values. This feature is consistent with the activated transverse components of velocity fluctuations observed in Chung et al. (2000). To assess the changes in the AIM, the maximum values of $-II$ and III are monitored. The maximum values of $-II$ and III at several streamwise locations are summarised in Tables 1 and 2. At $x = 15$, the maximum values of $-II$ and III in the blowing case are decreased by 13% and 21%, respectively. These values correspond to two thirds of the total decrease obtained at the exit of the computational domain. Further downstream (at $x = 30$), the effect of blowing on the anisotropy tensor is mild compared with the strong early response at $x = 15$.

It appears that the relaxation processes of the near-wall anisotropy in the blowing and suction cases are different from each other. In the suction case, the early response of the near-wall anisotropy is rather slow. At $x = 15$,

the AIM in the suction case does not change much from the inlet values as shown in Fig. 5. Further downstream (at $x = 30$), however, the turbulence becomes more anisotropic and the Reynolds stress tensor begins to approach a right-hand side vertex corresponding to the one-component turbulence. The maximum values of $-II$ and III at $x = 30$ are increased by 11% and 20%. The slow response of the anisotropy is also seen in the Reynolds stresses shown in Fig. 2.

It appears that the anisotropy tensor of near-wall turbulence approaches its asymptotic value near the exit. The near-wall value in the suction wall approaches a right-hand side vertex corresponding to the one-component turbulence. The maximum values of $-II$ and III in the suction case are very close to the coordinates of the top vertex (see Table 2). The maximum values of $-II$ and III decrease by 20% and 33% in the blowing case and increase by 15% and 27% in the suction case, respectively. This is fairly close to the asymptotic values obtained from the periodic DNS (Sumitani and Kasagi, 1985). In their DNS, the decrease in the blowing case was 22% and 36% and the increase was 14% and 24% in the suction case, compared to the no blowing/suction case.

Figure 6 shows the limiting behaviour of the Reynolds stresses at the blowing and suction wall, respectively. The relaxation process associated with blowing is faster than that with suction. All the components approach an equi-

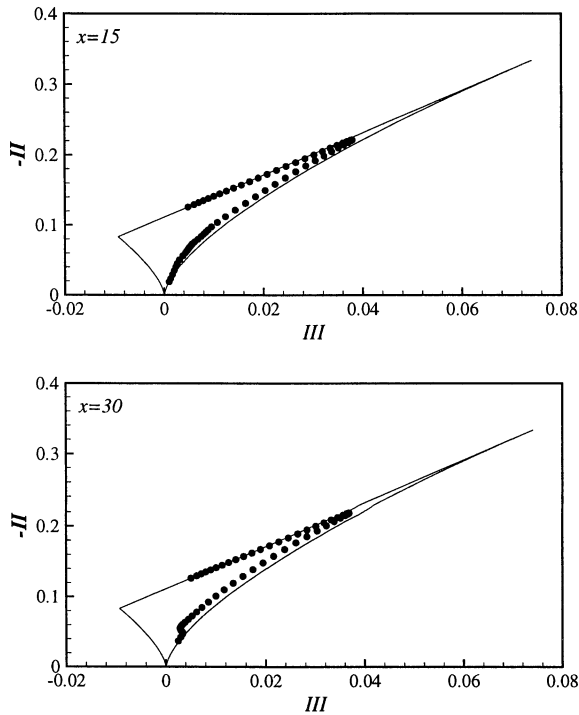


Figure 4: Anisotropy invariant map for blowing at a) $x = 15$ and b) $x = 30$.

librium state at around $x = 15$. Note that the limiting values at wall have a faster response than the velocity fluctuations themselves. The velocity fluctuations have an equilibrium state at around $x = 20$ (Chung et al. 2000). On the contrary, suction has a slow relaxation as shown in Fig. 6b).

CONCLUDING REMARKS

The anisotropy tensor obtained from direct numerical simulation data of a turbulent channel flow is analysed to investigate the modulation of the near-wall anisotropy with uniform wall blowing and suction. The previous findings which suggest the effects of wall blowing and suction on the near-wall turbulent structure are corroborated in the present study. It is found that blowing activates the transverse ($\overline{v'^2}$ and $\overline{w'^2}$) components of velocity fluctuations and decreases the anisotropy of the near-wall turbulence significantly. When suction is applied, turbulence becomes much more anisotropic and the near-wall values approach a right-hand side vertex in the AIM corresponding to the one-component turbulence. After the sudden application of wall blowing and suction, there is a delay in the response of the near-wall anisotropy to the sudden change. A study of the AIM indicates that the response of near-wall anisotropy to blowing is

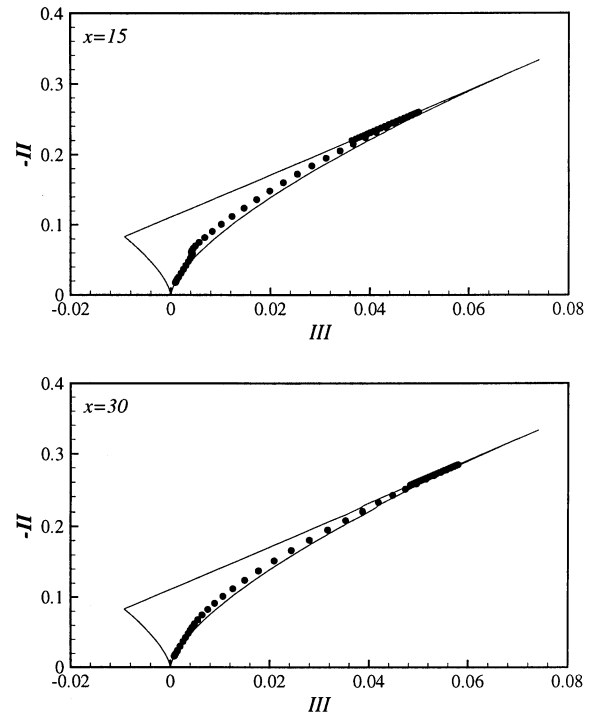


Figure 5: Anisotropy invariant map for suction at a) $x = 15$ and b) $x = 30$.

	$x = 0$	$x = 15$	$x = 30$	$x = 45$
$-II$	0.255	0.221	0.217	0.204
III	0.0484	0.0380	0.0367	0.0324

Table 1: Maximum values of $-II$ and III at several stream-wise locations in the blowing case.

	$x = 0$	$x = 15$	$x = 30$	$x = 45$
$-II$	0.255	0.260	0.284	0.295
III	0.0484	0.0498	0.0579	0.0614

Table 2: Maximum values of $-II$ and III at several stream-wise locations in the suction case.

faster than the response to suction.

ACKNOWLEDGEMENTS

The authors are grateful to Kyung-Soo Yang for assistance with computational aspects of this work and for permitting us to use his program. We also thank Per-Åge Krogstad for reading the manuscript. This research was supported partially by a grant from the National Research Laboratory of the Ministry of Science and Technology, Korea.

REFERENCES

- Antonia, R. A., Fulachier, L., Krishnamoorthy, L. V., Benabid, T., and Anselmet F., 1988, "Influence of wall suction on the organized motion in a turbulent boundary layer", *Journal of Fluid Mechanics*, Vol. 190, pp. 217–240.
- Antonia, R. A., Spalart, P. R., and Mar-

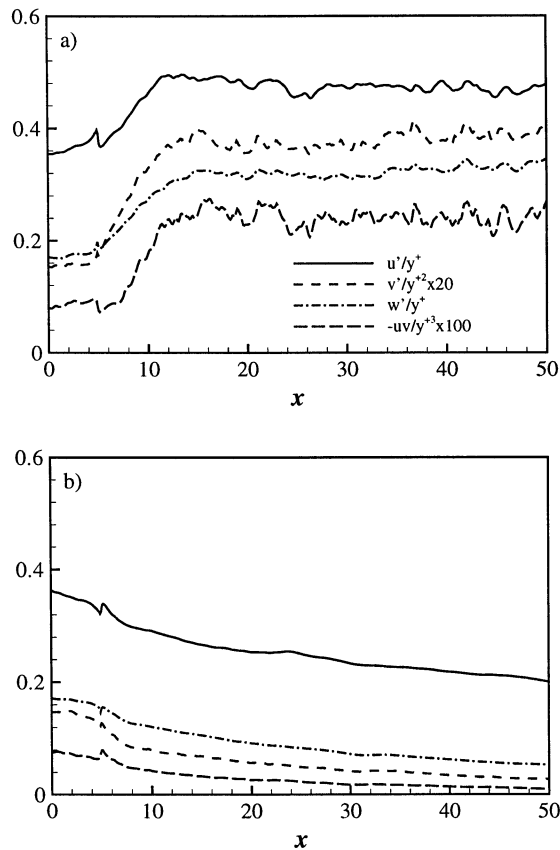


Figure 6: Distributions of the limiting behaviour of the Reynolds stresses. u^+/y^+ , $v^+/y^{+2} \times 20$, w^+/y^+ , $-\overline{uv}/y^{+3} \times 100$. a) at the blowing wall, and b) at the suction wall

iani, P., 1994, "Effect of suction on the near-wall anisotropy of a turbulent boundary layer", *Physics of Fluids*, Vol. 6, pp. 430–432.

Bushnell, D. M., and McGinley, C. B., 1989, "Turbulence control in wall flows", *Annual Review of Fluid Mechanics*, Vol. 21, pp. 1–20.

Chung, Y. M., and Sung, H. J., 1997, "Comparative Study of Inflow Conditions for Spatially Evolving Simulation", *AIAA Journal*, Vol. 35, pp. 269–274.

Chung, Y. M., and Sung, H. J., 1999, "Asymmetric response of turbulent channel flow to wall suction and blowing", In *Turbulence and Shear Flow -1*, (ed. S. Barnerjee and J. K. Eaton), pp. 423–428.

Chung, Y. M., and Sung, H. J., 2001, "Initial relaxation of spatially evolving turbulent channel flow subjected to wall blowing and suction", *AIAA Journal*, in press.

Chung, Y. M., Sung, H. J., and Luo, K. H., 2000, "Response of turbulent channel flow to sudden wall suction and blowing", In *8th European Turbulence Conference*, Barcelona, Spain.

Kim J., and Moin, P., 1985, "Application of a fractional-step method to incompressible Navier-Stokes equations", *Journal of Compu-*

tational Physics, Vol. 59, pp. 308–323.

Kim, J., Moin, P., and Moser, R., 1987, "Turbulent statistics in fully developed channel flow at low Reynolds number", *Journal of Fluid Mechanics*, Vol. 177, pp. 133–166.

Krogstad, P.-Å., and Kourakine, A., 2000, "Some effects of localized injection on the turbulent structure in a boundary layer", *Physics of Fluids*, Vol. 12, pp. 2990–2999.

Lumley, J. L., and Newman, G., 1979, "The return to isotropy of homogeneous turbulence", *Journal of Fluid Mechanics*, Vol. 82, pp. 161–178.

Mariani, P., Spalart, P. R., and Kollmann, W., 1993, "Direct simulation of a turbulent boundary layer with suction", *Near-Wall Turbulent Flows*, edited by R. M. C. So, C. G. Speziale, and B. E. Launder, Elsevier, Amsterdam, pp. 347–356.

Moin, P., 1982, "Numerical simulation of wall-bounded turbulent shear flows", In *proceedings of the 8th International Conference on Numerical Methods in Fluid Dynamics*, edited by E. Krause, Springer-Verlag, New York, pp. 55–76.

Park, J., and Choi, H., 1999, "Effects of uniform blowing or suction from a spanwise slot on a turbulent boundary layer flow", *Physics of Fluids*, Vol. 11, pp. 3095–3105.

Piomelli, U., Ferziger, J. H., and Moin, P., 1989, "New approximate boundary conditions for large eddy simulations of wall-bounded flows", *Physics of Fluids A*, Vol. 1, pp. 1061–1068.

Schildknecht, M., Miller, J. A., and Meier, G. E. A., 1979, "The influence of suction on the structure of turbulence in fully developed pipe flow", *Journal of Fluid Mechanics*, Vol. 90, pp. 67–107.

Simpson, R. L., 1971, "The effect of a discontinuity in wall blowing on the turbulent incompressible boundary layer", *International Journal of Heat and Mass Transfer*, Vol. 14, pp. 2083–2097.

Smits, A. J., and Wood, D. H., 1985, "The response of turbulent boundary layers to sudden perturbations", *Annual Review of Fluid Mechanics*, Vol. 17, pp. 321–358.

Sumitani Y., and Kasagi, N., 1995, "Direct numerical simulation of turbulent transport with uniform wall injection and suction", *AIAA Journal*, Vol. 33, pp. 1220–1228.

Yang K.-S., and Ferziger, J. H., 1993, "Large-eddy simulation of turbulent obstacle flow using a dynamic subgrid-scale model", *AIAA Journal*, Vol. 31, pp. 1406–1413.